Published in final edited form as:
Genes Chromosomes Cancer. 2014 July ; 53(7): 622–633. doi:10.1002/gcc.22172.

Distinct Transcriptional Signature and Immunoprofile of *CIC-DUX4*–Fusion Positive Round Cell Tumors Compared to *EWSR1*-Rearranged Ewing Sarcomas – Further Evidence Toward Distinct Pathologic Entities

Katja Specht[1,*], **Yun-Shao Sung**[2,*], **Lei Zhang**[2], **Günther H. S. Richter**[3], **Christopher D. Fletcher**[4,¥], and **Cristina R. Antonescu**[2,¥]

[1]Institute of Pathology, Technische Universität München, Munich, Germany

[2]Department of Pathology, Memorial Sloan-Kettering Cancer Center, New York, NY, USA

[3]Children's Cancer Research Center and Department of Pediatrics, Roman Herzog Comprehensive Cancer Research Center and Klinikum rechts der Isar, Technische Universität München, Munich, Germany

[4]Department of Pathology, Brigham and Women's Hospital, Boston, MA, USA

Abstract

Round cell sarcomas harboring *CIC-DUX4* fusions have recently been described as highly aggressive soft tissue tumors of children and young adults. Due to partial morphologic and immunohistochemical overlap with Ewing sarcoma (ES), *CIC-DUX4*-positive tumors have generally been classified as Ewing sarcoma-like and managed similarly, however, a systematic comparison at the molecular and immunohistochemical levels between these two groups has not yet been conducted. Based on an initial observation that *CIC-DUX4*-positive tumors show nuclear immunoreactivity for WT1 and ETS transcription factors, FLI1 and ERG, we performed a detailed immunohistochemical and molecular analysis including these markers, to further investigate the relationship between *CIC-DUX4* tumors and ES. The study group included 21 *CIC-DUX4*-positive sarcomas and 20 *EWSR1*-rearranged ES. Immunohistochemically, *CIC-DUX4* sarcomas showed membranous CD99 positivity in 18 (86%) cases, but only 5 (24%) with a diffuse pattern, while WT1 and FLI1 were strongly positive in all cases. ERG was positive in 18% of cases. All ES expressed CD99 and FLI1, while ERG positivity was only seen in *EWSR1-ERG* fusion positive ES. WT1 was negative in all ES. Expression profiling validated by q-PCR revealed a distinct gene signature associated with *CIC-DUX4* fusion, with upregulation of *ETS* transcription factors (*ETV4*, *ETV1* and *ETV5)* and *WT1*, among top overexpressed genes compared to ES, other sarcomas and normal tissue. In conclusion, the distinct gene signature and immunoprofile of *CIC-DUX4* sarcomas suggest a distinct pathogenesis from ES. The consistent WT1 expression may provide a useful clue in the diagnosis in the context of round cell sarcomas negative for *EWSR1*-rearrangement.

¥Corresponding Authors: Cristina R Antonescu, MD, Memorial Sloan-Kettering Cancer Center, Pathology Department, 1275 York Ave, New York, NY, antonesc@mskcc.org and Christopher D Fletcher, Brigham and Women's Hospital, Boston, MA, cfletcher@partners.org.
*These authors contributed equally to this work

Keywords

small blue round cell sarcoma; *CIC-DUX4*; WT1; Ewing Sarcoma

INTRODUCTION

According to the current WHO classification (Fletcher et al., 2013), round cell undifferentiated soft tissue sarcomas (round cell USTS) lack consistent genetic abnormalities and are characterized by relatively monotonous round to ovoid cytomorphology, with a high nuclear to cytoplasmic ratio and no distinct line of differentiation. As they most often resemble Ewing sarcoma (ES), for practical and treatment purposes, round cell USTS have been classified as 'Ewing sarcoma-like' or lumped within the Ewing sarcoma family of tumors. However, in contrast to classic ES, round cell USTS lack the pathognomonic translocations involving the *EWSR1* gene on chromosome 22 fused to a member of the *ETS* transcription factor family, namely *FLI1* (Delattre et al., 1992), *ERG* (Zucman et al., 1993; Sorensen et al., 1994), *ETV1* (Jeon et al., 1995), *ETV4* (Urano et al., 1996) or *FEV* (Peter et al., 1997), or similar translocations involving the *FUS* gene (*FUS-ERG* or *FUS-FEV*) (Shing et al., 2003), (Ng et al., 2007).

We and others recently described a series of USTS with primitive round cell morphology harboring a novel gene fusion, *CIC-DUX4*, resulting from either t(4;19)(q35;q13) or a t(10;19)(q26;q13) (Kawamura-Saito et al., 2006; Yoshimoto et al., 2009; Italiano et al., 2012; Graham et al., 2012; Choi et al., 2013). The genes involved in the fusion are *CIC*, a transcriptional repressor in chromosome band 19q13.1 and *DUX4*, a double homeobox transcription factor, located in either 4q35 or 10q26.3. Due to its aggressive clinical course and potential therapeutic implications, recognition of this recently defined subgroup of round cell USTS is important. However, the lack of any lineage-specific markers can make diagnosis and classification difficult. Focal and weak expression of CD99 has been the only consistently reported immunohistochemical finding in these tumors (Kawamura-Saito et al., 2006; Italiano et al., 2012; Choi et al., 2013). Molecular confirmation by either FISH or RT-PCR currently represents the gold standard to establish a definitive diagnosis of *CIC-DUX4* round cell sarcomas, yet these tests are presently offered only at few centers.

As no systematic study has so far attempted to investigate the pathogenetic relationship between *CIC-DUX4*-positive tumors and ES, we carried out a detailed comparative immunohistochemical and molecular analysis using global gene expression profiling and validated by quantitative RT-PCR techniques.

MATERIALS AND METHODS

The consultation files of the corresponding authors (CRA, CDF) and the Surgical Pathology files of Memorial Sloan Kettering Cancer Center, New York, NY (CRA) and the Technische Universität München, Germany (KS) were searched for diagnosis of small blue round cell tumors/sarcomas and Ewing sarcomas, with tissue available for further immunohistochemical and molecular analysis, between 2001–2012. A total of 33 round cell USTS lacking *EWSR1* gene rearrangements (or other common sarcoma-associated

translocations) were identified. Hematoxylin and eosin-stained slides and previously performed immunohistochemical stains were reviewed in all cases. Among the 33 round cell USTS, 21 (64%) cases harbored *CIC* gene rearrangements by FISH (Table 1), cases #1–6 being previously reported (Italiano et al., 2012). In addition, a comparison group of 20 Ewing sarcomas (ES) was used for immunohistochemical studies and validation q-PCR. The diagnosis of ES was confirmed by reverse transcriptase polymerase chain reaction (RT-PCR) and sequencing analysis in 11 cases, showing a *EWSR1-FLI1* in 9 cases and a *EWSR1-ERG* fusion transcript in 3 cases. Additional 9 cases showed *EWSR1* gene rearrangement by fluorescence in situ hybridization (FISH). One case was confirmed by both methodologies. All cases were handled in accordance with the ethical rules of the respective institutions.

Interphase FISH

FISH analysis was performed on interphase nuclei from paraffin-embedded 4 μm sections using bacterial artificial chromosomes (BAC clones), flanking *CIC* in 19q13 and *DUX4* in 4q35 and 10q26.3 as previously described (Italiano et al., 2012). Two hundred tumor nuclei were evaluated using a Zeiss fluorescence microscope (Zeiss Axioplan, Oberkochen, Germany), controlled by Isis 5 software (Metasystems). A cut-off of >20% nuclei showing a break-apart signal was considered to be positive for rearrangement. Nuclei with incomplete set of signals were omitted from the score.

Immunohistochemistry

Immunohistochemistry was performed on whole tissue sections of the 21 *CIC-DUX4* – positive round cell sarcoma cases and in the 20 cases of Ewing sarcoma using the following antibodies: an anti-CD99 mouse monoclonal antibody (1:150; clone O13, Covance), an anti-FLI1 mouse monoclonal antibody raised against a bacterially expressed FLI1 Ets domain fusion protein (1:100; G146-222, BD Bioscience), an anti-ERG rabbit monoclonal antibody raised against a synthetic peptide corresponding to the carboxy-terminal end of ERG (1:2000; EPR3864(2), Epitomics), and an anti-WT-1 mouse monoclonal antibody (1:50; 6F-H2, DAKO; which is directed at the N-terminal and reacts with all isoforms of the full-length WT1). Immunodetection was performed using the Envision Plus detection system (Dako). The extent of immunoreactivity was graded according to the percentage of positive tumor cells (0 <5% or no staining; 1+ 5– 25%; 2+ 26–50%; 3+ 51–75%, 4+ 76%–100%). The intensity of staining was graded as weak, moderate or strong.

Gene Expression Profiling

Total RNA from fresh-frozen tissue extracted from 5 *CIC-DUX4* positive tumors, two with t(4;19)(q35;q13) and three with t(10;19)(q26;q13) translocation, was labeled and hybridized onto an Affymetrix U133A chip (22,000 transcripts), as previously described (Antonescu et al., 2004). Their expression was compared to a previously published, well-characterized dataset of 29 soft tissue sarcomas (Segal et al., 2003; Hadju et al., 2010) and 8 normal tissues.

In parallel, we investigated 5 *EWSR1-FLI1* fusion positive ES tumors and 21 normal tissues using the Affymetrix Human Gene 1.0 ST arrays (32,000 transcripts); microarray data been previously deposited at the gene expression omnibus (GSE45544). The transcriptional

signature was further compared to a comprehensive gene expression meta-analysis of ES tumors (Hancock and Lessnick, 2008). The overlapping upregulated and downregulated 95 genes from the two analyses were selected and subsequently compared to the CIC-DUX4 signature (Fig. 3).

For the data analysis, RMA-normalization was performed, including background correlation, quantile normalization, and median polish summary method (Richter et al., 2009). Subsequent analysis was carried out with signal intensities that were log2-transformed to remove biases based on signal expression values (Hauer et al., 2013). Statistical t-test and FDR were performed to identify differentially expressed gene list, and subsequent hierarchical clustering was accomplished by heatmap function in R and bioconductor (Antonescu et al., 2009). Annotation files for Affymetrix U133A and Human Gene arrays were obtained from Affymetrix website (http://www.affymetrix.com/support/technical/annotationfilesmain.affx) and analyzed using PERL script in order to match the probe IDs. Subsequently, gene set enrichment analysis (GSEA) was performed for investigating statistical associations between variable gene sets and phenotype of interest (Wang and Cairns, 2013). The algorithm in GSEA calculates the enrichment score, with corresponding significance level based on permutation tests (empirical p-values and FDRs controlling global false positives). Each sample group was permutated 1,000 times to yield statistical significances.

Real-Time Quantitative RT-PCR (qPCR)

Total RNA was extracted from macrodissected formalin-fixed, paraffin-embedded tumor tissue using the High-Pure RNA Paraffin Kit reagent according to the manufacturer's instructions (Roche Diagnostics, Penzberg, Germany). One microgram of RNA was reverse transcribed into cDNA using Superscript II reverse transcriptase (Invitrogen) and 250 ng of random hexamers (Roche Diagnostics) in a final volume of 20 μl. Gene expression was assessed using RealTime ready single assays (Roche Diagnostics) for the target genes *ETV1* (ID 140599), *ETV4* (ID 137042), *ETV5* (ID 127143) and the housekeeping gene *ACTB* (ID 101125). Quantitative RT-PCR was performed in duplicate with the LightCycler 480 Instrument using LightCycler 480 Probes Master (Roche Diagnostics) and 10 ng of cDNA per well. Relative mRNA expression was calculated by the ΔΔCt method using the LightCycler 480 Software with normalization to ACTB as reference gene.

RESULTS

Clinicopathologic and Molecular Characteristics of *CIC-DUX4*-Fusion-Positive Round Cell Sarcomas

Among the 33 round cell USTS negative for *EWSR1*-associated gene fusions, a total of 21 tumors were positive for *CIC* gene rearrangements by FISH analysis (Table 1). Subsequent FISH analysis confirmed the fusion of *CIC* with the *DUX4* gene in either chromosome band 4q35 in 9 cases or in 10q26.3 in 6 cases. In 6 cases there was no abnormality identified in the two *DUX4* genes, suggesting alternative fusions events. In one *DUX4* negative tumor, the outside karyotype found a three-way translocation, t(2;10;19)(q35;p14;q13); the break on 2q35 being outside the *PAX3* locus by FISH (not shown). The cases affected 9 males and

12 females, with a mean and median age at diagnosis of 30 and 29, respectively (range 6–51 years). Five patients (24%) were younger than 20 years. Nineteen cases (90%) arose in somatic soft tissue, one tumor originated in the stomach and one patient presented with brain metastases, the primary tumor site being unknown. The anatomic distribution included upper extremity (3), lower extremity (5), trunk (9), head and neck (2) and stomach (1).

Microscopic Features

On microscopic examination, the *CIC-DUX4*-positive tumors were characterized by a diffuse or vaguely nodular growth of undifferentiated cells, arranged in solid sheets separated by thin fibrous septa or areas of necrosis (Fig. 1A, B). The majority of tumors exhibited infiltrative growth into adjacent anatomic structures, such as skeletal muscle or adipose tissue. Geographic tumor necrosis was common and prominent in the majority of cases, (15/21), with frequent apoptosis and individual tumor cell necrosis with a ‘starry-sky’ appearance or foci of pyknotic, ‘dark’ cells (Figs. 1A–C). The tumor cells contained small to medium-sized round to oval nuclei, with minor variability in size and shape, surrounded by variable amounts of amphophilic, clear or pale eosinophilic cytoplasm, typically more abundant than in ES (Fig. 1D). In contrast to classic ES, nuclei showed vesicular chromatin, with distinct and occasional prominent nucleoli (Figs. 1D, E). Mitotic counts ranged from 6–92 per 10 high-power fields (median count of 40). Some cases showed focally more prominent pleomorphism (Figs. 1D, E) and spindle cell areas (Fig. 1F). Patchy myxoid or edematous stromal change was frequently seen, sometimes with formation of microcystic spaces. No rosette formation was observed.

Immunohistochemical Findings

The results of the immunohistochemical studies are summarized in Table 1. Membranous CD99 staining was seen in 18/21 (86%) *CIC-DUX4*-positive cases (Fig. 2A). Staining was mostly focal and patchy (1+, <25% of the cells) with weak to moderate intensity, as seen in 13 (62%) cases. Three cases (14%) were completely negative for CD99. All cases tested were uniformly and strongly positive for Fli1 (9/9; Fig. 2B). ERG positivity was seen in 2 cases (2/11; 18%), with either focal (1+) and weak or multifocal (3+) and moderate intensity (Fig. 2C). WT-1 showed positivity in all cases tested (20/20), displaying mostly a combined nuclear and cytoplasmic pattern of staining, with moderate to strong intensity in 15/20 cases tested (Fig. 2D); 4 showed only nuclear staining, while one tumor had only cytoplasmic reactivity. All neural and neuroendocrine markers including S-100, GFAP, synaptophysin, chromogranin, as well as all myogenic markers and lymphoid markers tested were negative. Similarly, all epithelial markers were negative, except for one tumor displaying focal Cam5.2 positivity.

In the ES group, as expected, all tumors showed strong and diffuse membranous CD99 expression (20/20). Strong and diffuse Fli1 nuclear reactivity was equally seen in all *EWSR1-FLI1* (n=13) and *EWSR1-ERG* (n=2) positive ES. ERG positivity was only seen in the 2 *EWSR1-ERG* but not in *EWSR1-FLI1*-positive Ewing sarcomas (2/17; 17%). All Ewing tumors assessed were negative for WT1 (0/17).

Gene Expression Signature

We further explored the pathogenetic relationship between *CIC-DUX4*-positive sarcomas and ES by comparing their transcriptional profiles. The *CIC-DUX4* associated gene expression signature of two t(4;19) and three t(10;19) tumors was obtained by comparison with a wide spectrum of soft tissue tumors and normal tissues. By unsupervised clustering the *CIC-DUX4*-positive sarcomas grouped in a tight genomic cluster from all other sarcomas and normal samples, regardless of the fusion type (Fig. 3A). A 175 gene-list of differentially expressed genes were identified (fold change, FC, >1.4, FDR $p<0.05$); most of them 144/175 (82%) being over-expressed (Table 2). Interestingly, among the highest ranked upregulated genes were *CRF, corticotropin releasing hormone* and *VGF, VGF nerve growth factor inducible*. Other top up-regulated genes were *PEA* family members of *ets* transcription factors, *ETV4*, *ETV1* and *ETV5*, as well as other notable transcription factors with function in sarcomagenesis: *ZIC1*, *HEY1*, and *WT1 (*Table 2, Fig. 3). Additional overexpressed genes were involved either in neuronal (*neuronal pentraxin I/II*) or skeletal muscle (*DLK1)* function. Among the tyrosine kinase receptors, *TIE1 (tyrosine kinase with immunoglobulin-like and EGF-like domains 1)* was significantly upregulated.

By comparing 5 *EWSR1-FLI1* fusion-positive tumors with a large spectrum of normal tissues (FC >1.3 or FC<−1.3 and adjusted p-value (FDR) < 0.1) 854 differentially expressed genes were identified. In parallel, we obtained the transcriptional signature of ES from a previously published comprehensive meta-analysis of ES tumors and cell lines (Hancock and Lessnick, 2008). Subsequently, we cross-referenced the gene lists from these two analyses and obtained 95 overlapping genes, representative of ES signature (Supplementary Table 1), which was then validated by hierarchical clustering of the ES and normal samples (Fig. 3D). The robust 95 gene-list of ES was then cross-referenced to the 175 genes differentially expressed in *CIC-DUX4* sarcomas and there were only 2 common genes identified (Fig. 3A).

Using GSEA, the 175 *CIC-DUX4* gene-list and the 95 *EWSR1-FLI1* gene-signature to the *CIC-DUX4*-positive cohort and ES group, respectively, high normalized enrichment scores were obtained, of 2.15 and 1.89, respectively, as well as clustered as distinct genomic groups due to their unique signature list (Figs. 3B, D). In contrast, applying *CIC-DUX4* and *EWSR1-FLI1* signature to ES and SBRCT samples, respectively, the enrichment scores obtained were low, of −0.7 and 0.91, respectively (Figs. 3C, E); suggesting that these signatures do not correlate with the opposite phenotype.

Q-PCR Validation of Top Upregulated Genes

To validate the gene array results as well as screen a larger cohort of *CIC-DUX4*–positive tumors, real-time quantitative RT-PCR analysis of selected *ETV1*, *ETV4*, *ETV5* was performed in 8 *CIC-DUX4* sarcomas and in 11 ES tumors. Median mRNA expression levels (ratio of target gene/housekeeping gene) were *ETV1*: 0.32 (range 0.14–0.38), *ETV4*: 3.42 (range 1.22–7.15), and *ETV5* 1.54 (range 0.8–2.56) in *CIC-DUX*-positive cases and *ETV1*: 0.013 (range 0.001–0.04), *ETV4*: 0.002 (range 0.0005–0.01), and *ETV5* 0.051 (range 0.02–0.54) in ES, with no significant difference in *EWSR1-FLI1* and *EWSR1-ERG*-fusion positive cases (Fig. 4). Gene expression level of *ETV6*, another member of ETS family of

transcription members, performed as a control, was not significantly elevated in *CIC-DUX4* tumors as compared to ES (data not shown).

DISCUSSION

Round cell sarcomas harboring a t(4;19)(q35;q13) or a t(10;19)(q26;q13) with *CIC-DUX4* fusion are recently described aggressive tumors arising in soft tissues of children and young adults. Due to partial morphologic overlap with Ewing sarcoma (ES) and weak/patchy CD99 expression as the only consistent immunoprofile, they have been referred to as 'Ewing sarcoma-like', although they lack the pathognomonic canonical *EWSR1-ETS* translocation of ES. Whether the group of *CIC-DUX4*-positive round cell sarcomas represents a stand-alone category of tumors or a subgroup of the Ewing sarcoma family of tumors is still a matter of debate. In the present study we provide novel immunohistochemical and molecular genetic evidence that *CIC-DUX4*-positive sarcomas represent a pathologic entity distinct from ES.

The first case of sarcoma with a t(4;19)(q35;q13.1) as the sole cytogenetic abnormality was reported by Richkind et al (Richkind et al., 1996) in a 12 year-old boy, who presented with an ankle soft tissue mass and synchronous lung metastases and died of disease within 10 months. Ten years later, Kawamura-Saito et al. identified the genes *CIC* in chromosome band 19q13 and *DUX4* in 4q35 resulting from the t(4;19)(q35;q13) in two round cell sarcoma cases of adults (Kawamura-Saito et al., 2006). More recently, it has been shown that a *CIC-DUX4* fusion can result not only from a t(4;19)(q35;q13), but also from a t(10;19)(q26;q13); the *DUX4* retrogene being located within a D4Z4 repeat array in the subtelomeric regions of chromosome bands 4q35 and 10q26.3 (Italiano et al., 2012).

To our knowledge, 25 cases with a t(4;19) or a t(10;19) with *CIC-DUX4* fusion have been reported in the literature so far (Richkind et al., 1996; Somers et al., 2004; Kawamura-Saito et al., 2006; Yoshimoto et al., 2009; Graham et al., 2012; Italiano et al., 2012; Choi et al., 2013). Together with the 15 new cases described in the current series, the total number of patients with *CIC-DUX4*-positive sarcomas reported is expanded to 40. Combined clinicopathologic data indicate an almost equal gender distribution (male: female ratio = 1.08), a median age at diagnosis of 26 years (range 6–62 years), a tumor location within soft tissue (>95%), and a high rate of metastatic relapse (75% cases with available follow-up), with lung as the most frequent site of metastasis (65%).

Although *CIC-DUX4* round cell sarcomas have been classified under the umbrella of Ewing sarcoma family of tumors, emerging clinicopathologic immunohistochemical and genetic evidence suggest important differences. First, the anatomic distribution is different, with the majority of *CIC-DUX4*-sarcomas reported so far, including our series, occurring in the deep soft tissue of extremities and trunk, whereas typical ES presents much more common as a bone tumor. Second, the *CIC-DUX4*-positive tumors mainly affect young adults with a peak incidence in the third decade, with equal gender distribution. In contrast, patients with ES have a mean age at diagnosis of 15 years (Sankar and Lessnick, 2011), with a slight male predominance. Although both tumor entities share an undifferentiated and mostly monotonous cytomorphology, there are subtle but distinctive features associated with *CIC-*

DUX4-positive tumors, such as increased nuclear size and shape variability, vesicular chromatin with focally prominent nucleoli, in addition to more abundant cytoplasm. Myxoid matrix and prominent stromal edema, often present in *CIC-DUX4*-associated tumors, are usually not seen in ES. In contrast, neural differentiation, i.e. Homer-Wright rosettes, a distinctive if infrequent morphologic feature of primitive neuroectodermal tumor (PNET), are not observed in *CIC-DUX4*-positive sarcomas.

The immunophenotype of *CIC-DUX4*-associated tumors is also not identical with ES. Based on our immunohistochemical data, most *CIC-DUX4*-positive tumors show weak and patchy staining with CD99 (Somers et al., 2004; Kawamura-Saito et al., 2006; Rakheja et al., 2008; Yoshimoto et al., 2009; Italiano et al., 2012; Graham et al., 2012). In contrast, ES shows diffuse and strong membranous reactivity with CD99. The MIC*2* membrane-associated glycoprotein of ES cells is recognized by a number of monoclonal antibodies including 12E7, HBA71, O13, and HO36-1.1. Although CD99 immunopositivity has been documented in a significant subset of small blue round cell tumors (but mostly cytoplasmic, weak), including lymphoblastic leukemia and lymphoma (Riopel et al., 1994), rhabdomyosarcoma (Stevenson et al., 1994), poorly differentiated synovial sarcoma (Dei Tos et al., 1995), desmoplastic round cell tumor (Ordonez, 1998) and small cell osteosarcoma (Devaney et al., 1993), it continues to be an important and helpful marker in the diagnosis of ES.

WT1 staining was observed in all *CIC-DUX4*-positive tumors examined, with a diffuse (3+ or 4+) and moderate to strong nuclear or nuclear and cytoplasmic pattern. Only one case showed exclusively diffuse cytoplasmic staining (3+). In contrast, WT1 immunohistochemistry was negative in all ES tested (0/17), confirming previous reports of absence of WT1 staining in Ewing family of tumors (Barnoud et al., 2000). WT1 is a diagnostic immunomarker best known for its utility in the diagnosis of Wilms tumor, desmoplastic small round cell tumor and mesothelioma (Grubb et al., 1994; Amin et al., 1995; Charles et al., 1997). Due to its absence in ES, the use of WT1 antibody can help in the differential diagnosis with other small round cell tumors in the appropriate clinical, morphological and immunohistochemical context. Our finding of consistent WT1 immunoreactivity in *CIC-DUX4*-positive sarcomas may serve as a useful marker in the differential diagnosis of ES, when molecular confirmation is not available. WT1 protein overexpression is most likely due to its transcriptional upregulation (see below) and not secondary to genetic abnormalities or rearrangements of the *WT1* gene locus, excluded by *WT1* FISH in 8 *CIC*-rearranged tumors, including 6 of the 7 tumors lacking *DUX4* gene abnormalities (data not shown).

Based on our initial observation of *FLI1* and *ERG* immunoreactivity in cases of *CIC-DUX4* sarcomas, we systematically examined the expression of these two markers in this series. Anti-FLI1 antibody labeled all eight *CIC-DUX4* cases with a diffuse and strong labeling pattern (8/8). Similarly, diffuse and strong nuclear FLI1 expression was present in the 15 ES investigated, regardless of fusion type. The latter findings are similar to those of Folpe et al. (Folpe et al., 2000) and Wang et al. (Wang et al., 2012) who also found strong FLI1 expression in ES, regardless of its *EWSR1* fusion partner. As noted previously (Wang et al., 2012), one possible explanation for this phenomenon is the cross-reactivity of FLI1 antibody

with the highly conserved and homologous Ets DNA binding domain present in the C-terminus of both FLI and ERG. Whether strong FLI1 expression observed in *CIC-DUX4* sarcoma reflects 'true' FLI1 protein overexpression or activation of related Ets proteins remains debatable; our gene expression data from *CIC-DUX4*-sarcomas, however, favors the latter possibility. Using a specific anti-ERG monoclonal antibody, ERG positivity was demonstrated in 2/11 *CIC-DUX4* sarcoma cases (18%), with either focal (1+) and weak, or multifocal (3+) with moderate intensity. In comparison, strong ERG staining was only seen in *EWSR1-ERG*-positive Ewing sarcoma (2/2; 100%), but not in *EWSR1-FLI1*-positive Ewing sarcoma (0/15).

Finally, the molecular genetic abnormalities of *CIC-DUX4*-positive sarcomas are different from Ewing sarcoma family tumors. ES tumors harbor the canonical fusion between *EWSR1* and *ETS* family members; the resulting chimeric genes encode aberrant transcription factors that play a crucial role in their pathogenesis (Sankar and Lessnick, 2011). In contrast, *CIC-DUX4* fusion appears functionally unrelated to *EWSR1-ETS. CIC* is the human homologue of *Drosophila capicua*, a gene identified in a screen for mutations affecting the anterior-posterior pattern of *Drosophila* embryos (Jimenez et al., 2000). It encodes a transcriptional repressor with a high-mobility group (HMG)-box containing DNA binding domain. *CIC* gene abnormalities have been implicated in neoplasia - for example, *CIC* loss of function mutations are identified in 83% of oligodendrogliomas (Bettegowda et al., 2011, Sahm et al., 2012). The *DUX4* gene is normally expressed in germ cells and is epigenetically silenced in somatic differentiated tissues. Aberrant expression of DUX4 has been implicated in the development of facioscapulohumeral muscular dystrophy (van der Maarel et al., 2011).

Despite different and functionally unrelated genes involved in the translocation, a possible pathogenetic link between *CIC-DUX4* sarcoma and Ewing family of tumors is suggested by our gene expression results. Although the transcriptional profile of *CIC-DUX4*-positive sarcomas is distinct from that of ES and other sarcoma subtypes, in keeping with them being separate tumor entities, *CIC-DUX4* fusion overexpresses three *ETS* transcription factors (*ETV4*, *ETV1* and *ETV5)* from the *PEA3* (polyoma enhancer activator 3) subfamily (Sankar and Lessnick, 2011). Thus, up-regulation of the *PEA3* family genes by CIC-DUX4 could serve as an equivalent molecular change to the *EWSR1-ETS* fusion. Interestingly, *ETV1* and *ETV4* can serve as fusion partners to *EWSR1* in rare cases of ES (Sankar and Lessnick, 2011). In analogy to *EWS/ETS* fusion-positive Ewing sarcoma, one might speculate that *CIC-DUX4* fusion induces an aberrant transcriptional program with deregulation of overlapping/converging or functionally similar key oncogenic target genes, thereby sharing a basic pathogenesis with Ewing sarcoma. It is of interest in this context that 92% of the reported ES rare variant translocations (*EWSR1-ETV1*, *EWSR1-ETV4* or *EWSR1-FEV)* occurred at extraskeletal sites (Wang et al., 2007). Whether this is a reporting bias or represents a specific feature of these rare translocation variants remains undetermined at this time. Our study confirms and extends the previous report of upregulation of *ETV5* and *ETV1* (but not of *ETV4*) genes by *CIC-DUX4* fusion (Kawamura-Saito et al., 2006). Using an experimental cell line model system, Kawamura-Saito et al. demonstrated binding of the HMG-box of CIC to a DNA sequence within the promoter of *PEA* genes *ETV1* and *ETV5*. Their results further revealed that fusion of *DUX4* to *CIC* sequence provides strong

transcriptional activity, resulting in mostly upregulated gene expression, with minimal down-regulated genes, in keeping with our own results.

Apart from *ETS* family members, other genes upregulated in *CIC-DUX4*-positive sarcomas include transcription factors such as *HMGA2, ZIC1, HEY1 and WT1*, previously shown to play a pathogenetic role in other sarcoma types. There was no transcriptional overlap between the CIC-DUX4 and ES gene expression signature.

In summary, *CIC-DUX4*-positive round cell sarcomas have a unique clinical presentation, morphology, immunoprofile and genetic signature that are different from ES. *CIC-DUX4*-positive sarcomas occur almost exclusively in deep soft tissue of young adults. The immunoprofile comprises weak and focal CD99 reactivity and diffuse nuclear WT1. Frequent FLI1 and occasional ERG immunoreactivity observed in *CIC-DUX4* sarcoma are similarly seen in ES. The gene signature of *CIC-DUX4*-positive sarcomas separates them from classic ES and justifies designation as a “stand alone” category.

Supplementary Material

Refer to Web version on PubMed Central for supplementary material.

Acknowledgments

Supported in part by: Wilhelm-Sander-Stiftung (KS), TransSaRNet; 01GM1104B of the BMBF, Germany (GHSR), P01CA47179 (CRA), P50 CA 140146-01 (CRA), Kristen Ann Carr Fund (CRA).

We thank Brigit Geist for expert technical assistance and Milagros Soto for excellent editorial assistance.

References

Amin KM, Litzky LA, Smythe WR, Mooney AM, Morris JM, Mews DJ, Pass HI, Kari C, Rodeck U, Rauscher FJ, Kaiser LR, Albelda SM. Wilms’ tumor 1 susceptibility (WT1) gene products are selectively expressed in malignant mesothelioma. Am J Pathol. 1995; 146:344–356. [PubMed: 7856747]

Antonescu CR, Viale A, Sarran L, Tschernyavsky SJ, Gonen M, Segal NH, Maki RG, Socci ND, DeMatteo RP, Besmer P. Gene expression in gastrointestinal stromal tumors is distinguished by KIT genotype and anatomic site. Clin Cancer Res. 2004; 10:3282–3290. [PubMed: 15161681]

Antonescu CR, Yoshida A, Guo T, Chang NE, Zhang L, Agaram NP, Qin LX, Brennan MF, Singer S, Maki RG. KDR activating mutations in human angiosarcomas are sensitive to specific kinase inhibitors. Cancer Res. 2009; 69:7175–7179. [PubMed: 19723655]

Barnoud R, Sabourin JC, Pasquier D, Ranchere D, Bailly C, Terrier-Lacombe MJ, Pasquier B. Immunohistochemical expression of WT1 by desmoplastic small round cell tumor: a comparative study with other small round cell tumors. Am J Surg Pathol. 2000; 24:830–836. [PubMed: 10843285]

Bettegowda C, Agrawal N, Jiao Y, Sausen M, Wood LD, Hruban RH, Rodriguez FJ, Cahill DP, McLendon R, Riggins G, Velculescu VE, Oba-Shinjo SM, Marie SK, Vogelstein B, Bigner D, Yan H, Papadopoulos N, Kinzler KW. Mutations in CIC and FUBP1 contribute to human oligodendroglioma. Science. 2011; 333:1453–1455. [PubMed: 21817013]

Charles AK, Moore IE, Berry PJ. Immunohistochemical detection of the Wilms’ tumour gene WT1 in desmoplastic small round cell tumour. Histopathology. 1997; 30:312–314. [PubMed: 9147076]

Choi EY, Thomas DG, McHugh JB, Patel RM, Roulston D, Schuetze SM, Chugh R, Biermann JS, Lucas DR. Undifferentiated Small Round Cell Sarcoma With t(4;19)(q35;q13.1) CIC-DUX4

Fusion: A Novel Highly Aggressive Soft Tissue Tumor With Distinctive Histopathology. Am J Surg Pathol. 2013; 37:1379–1386. [PubMed: 23887164]

Dei Tos AP, Wadden C, Calonje E, Sciot R, Pauwels P, Knight JC, Dal Cin P, CDF. Immunohistochemical demonstration of gylcoprotein p30/32(MIC2) (CD99) in synovial sarcoma: a potential cause of diagnostic confusion. Applied Immunohistochemistry. 1995; 3:168–173.

Delattre O, Zucman J, Plougastel B, Desmaze C, Melot T, Peter M, Kovar H, Joubert I, de Jong P, Rouleau G, et al. Gene fusion with an ETS DNA-binding domain caused by chromosome translocation in human tumours. Nature. 1992; 359:162–165. [PubMed: 1522903]

Devaney K, Vinh TN, Sweet DE. Small cell osteosarcoma of bone: an immunohistochemical study with differential diagnostic considerations. Hum Pathol. 1993; 24:1211–1225. [PubMed: 7503935]

Fletcher, CDM. World Health Organization., International Agency for Research on Cancer. WHO classification of tumours of soft tissue and bone. 4. Lyon: IARC Press; 2013. p. 468

Folpe AL, Hill CE, Parham DM, O'Shea PA, Weiss SW. Immunohistochemical detection of FLI-1 protein expression: a study of 132 round cell tumors with emphasis on CD99-positive mimics of Ewing's sarcoma/primitive neuroectodermal tumor. Am J Surg Pathol. 2000; 24:1657–1662. [PubMed: 11117787]

Graham C, Chilton-MacNeill S, Zielenska M, Somers GR. The CIC-DUX4 fusion transcript is present in a subgroup of pediatric primitive round cell sarcomas. Hum Pathol. 2012; 43:180–189. [PubMed: 21813156]

Grubb GR, Yun K, Williams BR, Eccles MR, Reeve AE. Expression of WT1 protein in fetal kidneys and Wilms tumors. Lab Invest. 1994; 71:472–479. [PubMed: 7967503]

Hadju M, Singer S, Maki RG, Schwartz G, Keohan M, Antonescu CR. IGF2 over-expression in solitary fibrous tumours is independent of anatomical location and is related to loss of imprinting. J Pathol. 2010; 221:300–307. [PubMed: 20527023]

Hancock JD, Lessnick SL. A transcriptional profiling meta-analysis reveals a core EWS-FLI gene expression signature. Cell Cycle. 2008; 7:250–256. [PubMed: 18256529]

Hauer K, Calzada-Wack J, Steiger K, Grunewald TG, Baumhoer D, Plehm S, Buch T, Prazeres da Costa O, Esposito I, Burdach S, Richter GH. DKK2 mediates osteolysis, invasiveness, and metastatic spread in Ewing sarcoma. Cancer Res. 2013; 73:967–977. [PubMed: 23204234]

Italiano A, Sung YS, Zhang L, Singer S, Maki RG, Coindre JM, Antonescu CR. High prevalence of CIC fusion with double-homeobox (DUX4) transcription factors in EWSR1-negative undifferentiated small blue round cell sarcomas. Genes Chromosomes Cancer. 2012; 51:207–218. [PubMed: 22072439]

Jeon IS, Davis JN, Braun BS, Sublett JE, Roussel MF, Denny CT, Shapiro DN. A variant Ewing's sarcoma translocation (7;22) fuses the EWS gene to the ETS gene ETV1. Oncogene. 1995; 10:1229–1234. [PubMed: 7700648]

Jimenez G, Guichet A, Ephrussi A, Casanova J. Relief of gene repression by torso RTK signaling: role of capicua in Drosophila terminal and dorsoventral patterning. Genes Dev. 2000; 14:224–231. [PubMed: 10652276]

Kawamura-Saito M, Yamazaki Y, Kaneko K, Kawaguchi N, Kanda H, Mukai H, Gotoh T, Motoi T, Fukayama M, Aburatani H, Takizawa T, Nakamura T. Fusion between CIC and DUX4 up-regulates PEA3 family genes in Ewing-like sarcomas with t(4;19)(q35;q13) translocation. Hum Mol Genet. 2006; 15:2125–2137. [PubMed: 16717057]

Ng TL, O'Sullivan MJ, Pallen CJ, Hayes M, Clarkson PW, Winstanley M, Sorensen PH, Nielsen TO, Horsman DE. Ewing sarcoma with novel translocation t(2;16) producing an in-frame fusion of FUS and FEV. J Mol Diagn. 2007; 9:459–463. [PubMed: 17620387]

Ordonez NG. Desmoplastic small round cell tumor: II: an ultrastructural and immunohistochemical study with emphasis on new immunohistochemical markers. Am J Surg Pathol. 1998; 22:1314–1327. [PubMed: 9808124]

Peter M, Couturier J, Pacquement H, Michon J, Thomas G, Magdelenat H, Delattre O. A new member of the ETS family fused to EWS in Ewing tumors. Oncogene. 1997; 14:1159–1164. [PubMed: 9121764]

Rakheja D, Goldman S, Wilson KS, Lenarsky C, Weinthal J, Schultz RA. Translocation (4;19)(q35;q13.1)-associated primitive round cell sarcoma: report of a case and review of the literature. Pediatr Dev Pathol. 2008; 11:239–244. [PubMed: 17990934]

Richkind KE, Romansky SG, Finklestein JZ. t(4;19)(q35;q13.1): a recurrent change in primitive mesenchymal tumors? Cancer Genet Cytogenet. 1996; 87:71–74. [PubMed: 8646746]

Richter GH, Plehm S, Fasan A, Rossler S, Unland R, Bennani-Baiti IM, Hotfilder M, Lowel D, von Luettichau I, Mossbrugger I, Quintanilla-Martinez L, Kovar H, Staege MS, Muller-Tidow C, Burdach S. EZH2 is a mediator of EWS/FLI1 driven tumor growth and metastasis blocking endothelial and neuro-ectodermal differentiation. Proc Natl Acad Sci U S A. 2009; 106:5324–5329. [PubMed: 19289832]

Riopel M, Dickman PS, Link MP, Perlman EJ. MIC2 analysis in pediatric lymphomas and leukemias. Hum Pathol. 1994; 25:396–399. [PubMed: 8163272]

Sahm F, Koelsche C, Meyer J, Pusch S, Lindenberg K, Mueller W, Herold-Mende C, von Deimling A, Hartmann C. CIC and FUBP1 mutations in oligodendrogliomas, oligoastrocytomas and astrocytomas. Acta Neuropathol. 2012; 123:853–860. [PubMed: 22588899]

Sankar S, Lessnick SL. Promiscuous partnerships in Ewing's sarcoma. Cancer Genet. 2011; 204:351–365. [PubMed: 21872822]

Segal NH, Pavlidis P, Antonescu CR, Maki RG, Noble WS, DeSantis D, Woodruff JM, Lewis JJ, Brennan MF, Houghton AN, Cordon-Cardo C. Classification and subtype prediction of adult soft tissue sarcoma by functional genomics. Am J Pathol. 2003; 163:691–700. [PubMed: 12875988]

Shing DC, McMullan DJ, Roberts P, Smith K, Chin SF, Nicholson J, Tillman RM, Ramani P, Cullinane C, Coleman N. FUS/ERG gene fusions in Ewing's tumors. Cancer Res. 2003; 63:4568–4576. [PubMed: 12907633]

Somers GR, Shago M, Zielenska M, Chan HS, Ngan BY. Primary subcutaneous primitive neuroectodermal tumor with aggressive behavior and an unusual karyotype: case report. Pediatr Dev Pathol. 2004; 7:538–545. [PubMed: 15547779]

Sorensen PH, Lessnick SL, Lopez-Terrada D, Liu XF, Triche TJ, Denny CT. A second Ewing's sarcoma translocation, t(21;22), fuses the EWS gene to another ETS-family transcription factor, ERG. Nat Genet. 1994; 6:146–151. [PubMed: 8162068]

Stevenson AJ, Chatten J, Bertoni F, MM. CD99 (p30/32MIC2) neuroectodermal/Ewing's sarcoma antigen as an immunohistochemical marker: review of more than 600 tumors and the literature experience. Applied Immunohistochemistry. 1994; 2:231–240.

Urano F, Umezawa A, Hong W, Kikuchi H, Hata J. A novel chimera gene between EWS and E1A-F, encoding the adenovirus E1A enhancer-binding protein, in extraosseous Ewing's sarcoma. Biochem Biophys Res Commun. 1996; 219:608–612. [PubMed: 8605035]

van der Maarel SM, Tawil R, Tapscott SJ. Facioscapulohumeral muscular dystrophy and DUX4: breaking the silence. Trends Mol Med. 2011; 17:252–258. [PubMed: 21288772]

Wang L, Bhargava R, Zheng T, Wexler L, Collins MH, Roulston D, Ladanyi M. Undifferentiated small round cell sarcomas with rare EWS gene fusions: identification of a novel EWS-SP3 fusion and of additional cases with the EWS-ETV1 and EWS-FEV fusions. J Mol Diagn. 2007; 9:498–509. [PubMed: 17690209]

Wang WL, Patel NR, Caragea M, Hogendoorn PC, Lopez-Terrada D, Hornick JL, Lazar AJ. Expression of ERG, an Ets family transcription factor, identifies ERG-rearranged Ewing sarcoma. Mod Pathol. 2012; 25:1378–1383. [PubMed: 22766791]

Wang X, Cairns MJ. Gene set enrichment analysis of RNA-Seq data: integrating differential expression and splicing. BMC Bioinformatics. 2013; 14(Suppl 5):S16. [PubMed: 23734663]

Yoshimoto M, Graham C, Chilton-MacNeill S, Lee E, Shago M, Squire J, Zielenska M, Somers GR. Detailed cytogenetic and array analysis of pediatric primitive sarcomas reveals a recurrent CIC-DUX4 fusion gene event. Cancer Genet Cytogenet. 2009; 195:1–11. [PubMed: 19837261]

Zucman J, Melot T, Desmaze C, Ghysdael J, Plougastel B, Peter M, Zucker JM, Triche TJ, Sheer D, Turc-Carel C, et al. Combinatorial generation of variable fusion proteins in the Ewing family of tumours. Embo J. 1993; 12:4481–4487. [PubMed: 8223458]

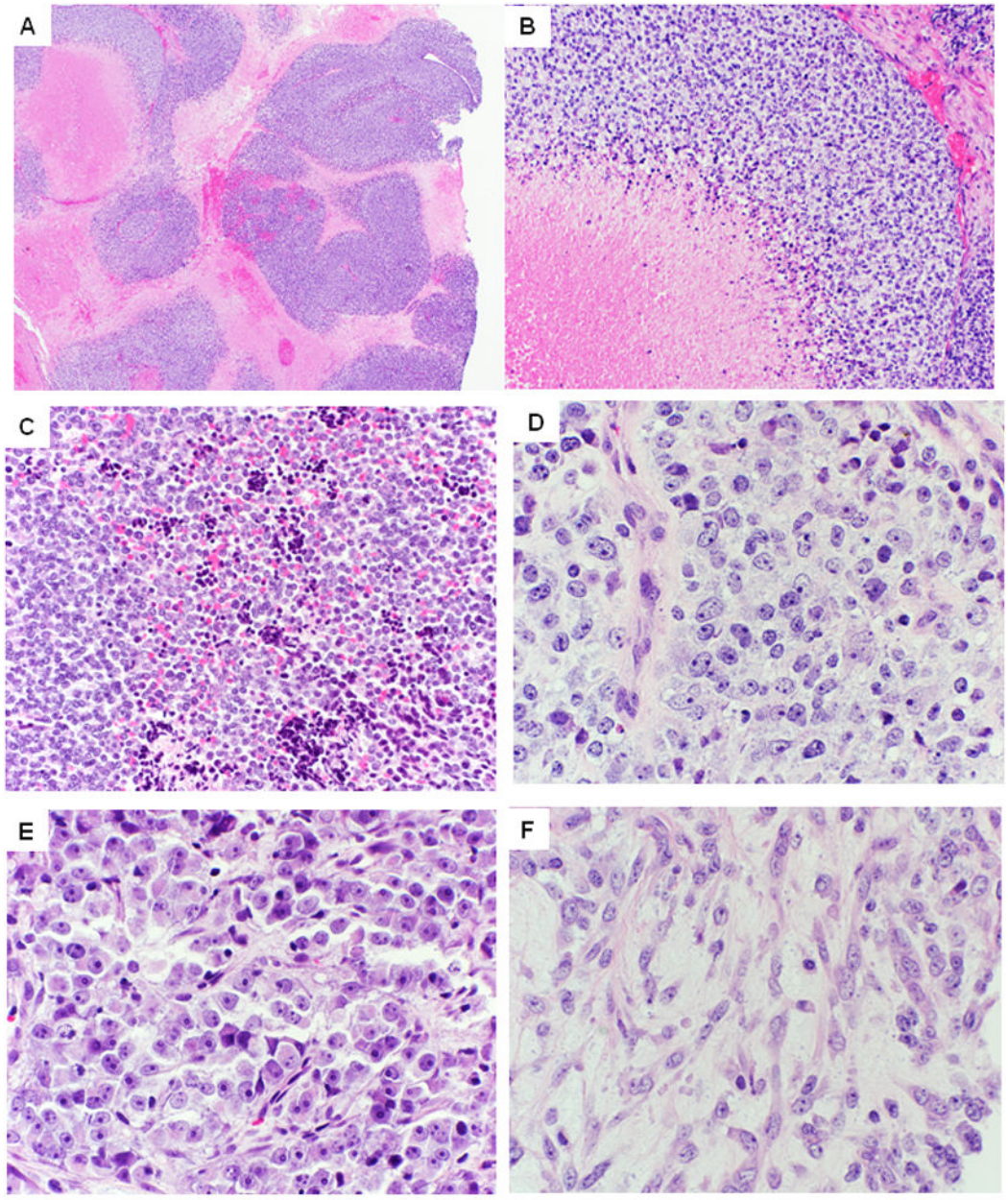

Figure 1. Pathologic features of *CIC-DUX4*-positive sarcomas

A. At low-power, tumors show a vague nodular growth, often outlined by confluent geographic areas of necrosis (case 10)

B. Higher power show tumor cells arranged in solid sheets, surrounding areas of necrosis (case 18).

C. Admixed with viable cells are often pyknotic, degenerating cells (case 20; x100).

D. Higher power showing ill-defined cell borders with vesicular chromatin and distinct nucleoli. Of note the nuclei show a round, oval to more angulated appearance, with subtle but increased pleomorphism than typical ES (case 16; x200).

E. Case 10 displaying greater variability in nuclear size, prominent nucleoli and more abundant cytoplasm, pushing the nuclei at the periphery.

F. Areas with spindle cell morphology are typically rare and present as a focal phenomenon. However, not uncommon is the presence of a edematous, myxoid stroma (case 16; 200x).

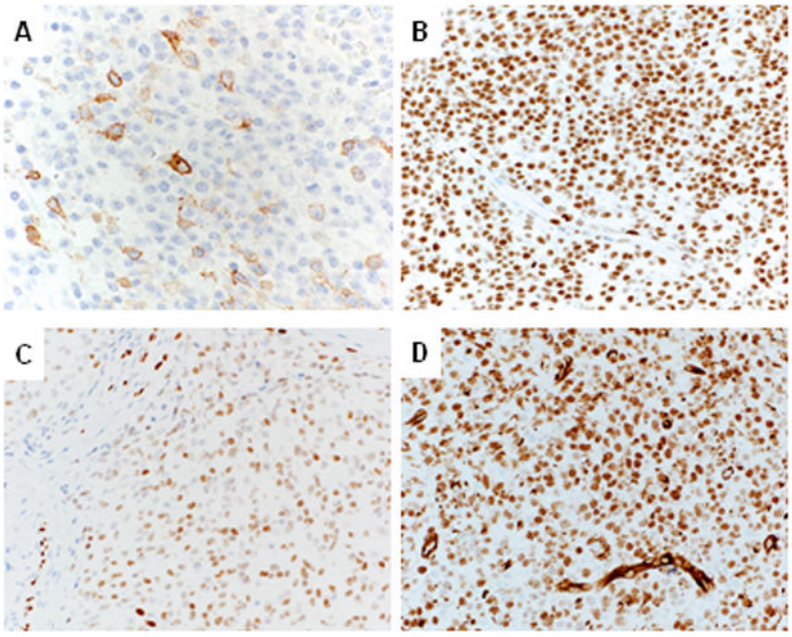

Figure 2. Immunohistochemical findings in *CIC-DUX4* sarcoma

A. CD99 expression is typically focal (1+) and of moderate intensity (case 16).

B. FLI1 labeling is uniformly strongly positive in the majority of tumor cells (case 16).

C. ERG expression is variable, with multifocal (3+) and moderate staining intensity (case 10).

D. WT-1 staining is seen in all *CIC-DUX4* – positive sarcomas, with most cases displaying both cytoplasmic and nuclear staining (case 10).

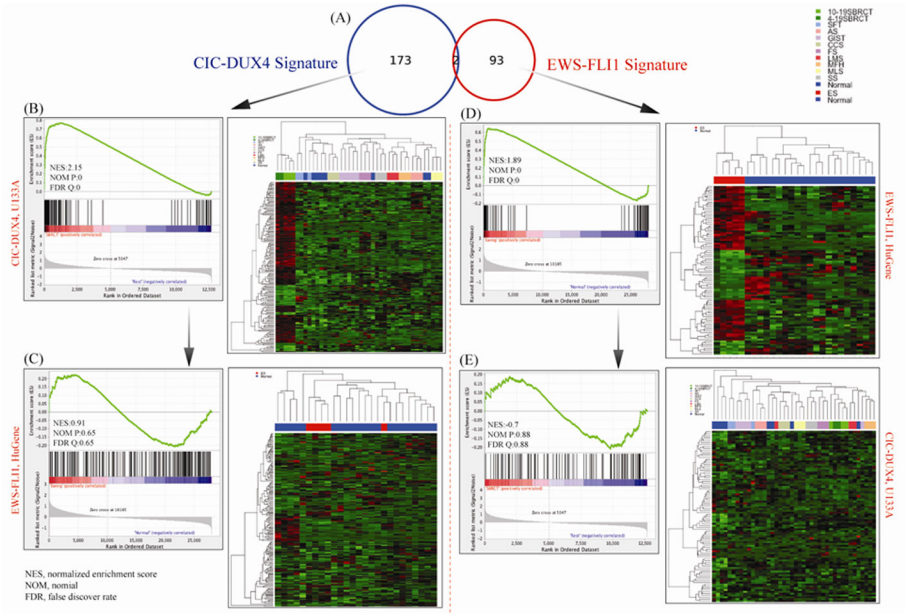

Fig. 3. Distinct Transcriptional Signature of *CIC-DUX4*-positive tumors compared to *EWSR1-FLi1* Ewing sarcoma (ES) cases

A. Venn diagram showing minimal genomic overlap between the two groups investigated (n=2 genes). The 175 gene list was obtained by comparing 5 *CIC-DUX4* tumors with 29 soft tissue sarcomas and 8 normal tissues on Affymetrix U133A chip (1.4 FC; FDR 0.05 p-value). The ES 95 gene-signature was obtained by overlapping the 854 differentially expressed genes in the 5 ES tumors (Affymetrix Hu-Gene; 1.3FC; FDR 0.1 p-value) with a published meta-analysis of ES. B. The 175 gene-signature was applied for hierarchical clustering showing a distinct genomic group of CIC-DUX4-tumors from all the other control samples. The GSEA confirms highly ranked genes, with high normalized enrichment score (NES) values. C. In contrast, applying the 175 *CIC-DUX4* gene-signature to the ES and controls resulted in poor clustering expression patterns and low GSEA scores. D. Hierarchical clustering using the robust 95 ES gene-list shows a well-defined ES genomic cluster from all the normal controls, with high NES scores on GSEA. E. In contrast, using the same 95 gene-signature on the *CIC-DUX4* tumors and controls shows an ambiguous expression pattern on clustering and low NEM score.

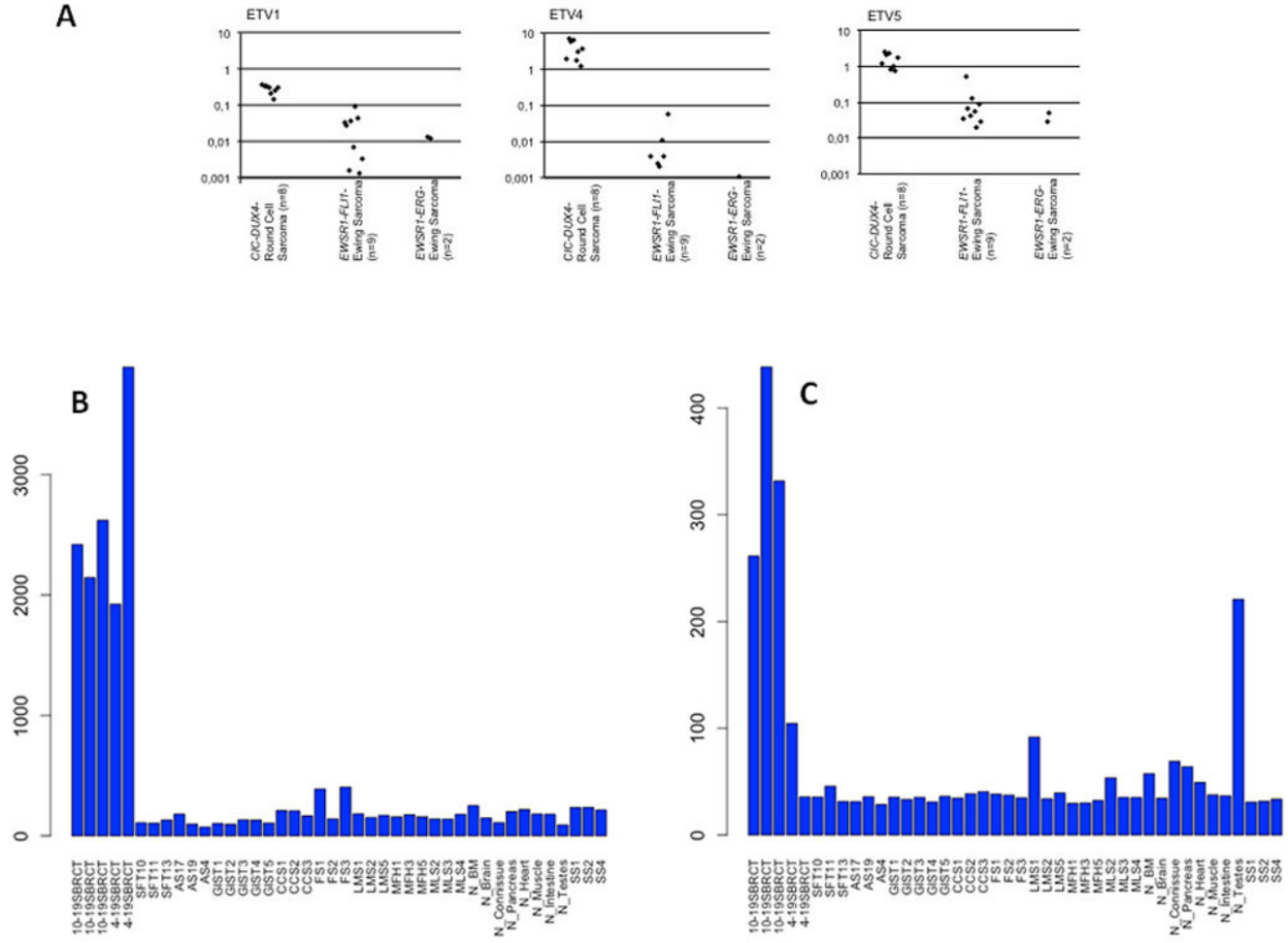

Fig. 4.

A. Quantitative RT-PCR reveals upregulation of *ETV1*, *ETV4* and *ETV5* in *CIC-DUX4* sarcomas (n=8) as compared to *EWSR1-FLI1* (n=9) or *EWSR1-ERG* (n=2) rearranged Ewing sarcomas (median *ETV1*: 24xfold; median *ETV4*: 1720x-fold; median *ETV5*: 30x-fold upregulation). B, C. Bar chart of mRNA overexpression of ETV4 (B) and WT1 (C) in CIC-DUX4-postiive tumors compared to other sarcoma types and normal tissue. WT1 shows overexpression mainly in the t(10;19) tumors.

Table 1

Clinical and Immunohistochemical Findings of CIC-rearranged Round Cell Sarcoma

Case#	Age/ Gender	Location	FISH for DUX4 on 4q35/10q26	CD99	Fli1	ERG	WT1
1	45/M	Back	t(10;19) CIC-DUX4	1+	4+	Neg	4+(N+C)
2	49/M	Arm	t(10;19) CIC-DUX4	3+	4+	Neg	4+(N+C)
3	30/F	Mandible	t(4;19) CIC-DUX4	3+	4+	Neg	4+(N+C)
4	29/F	Arm	t(10;19) CIC-DUX4	1+	ND	ND	2+(C)
5	28/M	Thigh	t(4;19) CIC-DUX4	3+	ND	ND	4+(N+C)
6	26/M	Arm	t(10;19) CIC-DUX4	3+	ND	ND	ND
7	36/F	Paraspinal	t(4;19) CIC-DUX4	1+	3+	Neg	2+(N)
8	19/F	Stomach	t(4;19) CIC-DUX4	3+	4+	Neg	4+(N)
9	25/M	Neck	t(4;19) CIC-DUX4	1+	ND	ND	4+(N+C)
10	51/F	Ankle	Neg	1+	ND	3+	4+(N+C)
11	14/F	Thigh	Neg	Neg	4+	Neg	4+(N+C)
12	27/F	Brain mets	Neg	1+	4+	Neg	4+(N+C)
13	50/F	Peritoneum	t(10;19) CIC-DUX4	1+	ND	ND	4+(N+C)
14	33/F	Knee	t(10;19) CIC-DUX4	Neg	ND	ND	4+(N+C)
15	36/F	Shoulder	t(4;19) CIC-DUX4	1+	ND	ND	4+(N+C)
16	13/F	Paravertebral	Neg	1+	4+	1+	4+(N+C)
17	25/F	Paravertebral	t(4;19) CIC-DUX4	1+	4+	Neg	4+(N+C)
18	47/M	Clavicular	t(4;19) CIC-DUX4	1+	ND	ND	4+(N+C)
19	37/M	Peri-prostatic	t(4;19) CIC-DUX4	1+	ND	Neg	4+(N+C)
20	6/M	Buttock	Neg*	1+	ND	ND	3+(N)
21	6/M	Scalp	Neg	Neg	ND	ND	3+(N)

M, male; F, female; N, nuclear, C, cytoplasmic; ND, not done, Neg, negative. Cases previously reported in ((Italiano et al., 2012): their case # 2,6,8,9,11,12); cases 1–3 and 6,7 were studied on U133A chip;

*case showed a karyotype of t(2;10;19)(q35;p14;q13)

Table 2

CIC-DUX4 Associated transcriptional signature[Ω]

Gene Symbol	U133A Probe ID	Chromosomal Location	Gene Ontology Molecular Function	Gene Title	Log FC	p-value
CRH	205629_s_at	chr8q13	hormone activity	corticotropin releasing hormone	4.8	0.006
NPTX2	213479_at	chr7q21.3-q22.1	metal ion binding	neuronal pentraxin II	4.2	0.005
ETV4[a]	211603_s_at	chr17q21	sequence-specific DNA binding transcription factor activity	ets variant 4	4.0	4.75E-05
HMGA2	208025_s_at	chr12q15	nucleic acid binding transcription factor activity	high mobility group AT-hook 2	4.0	2.25E-05
DUSP4	204014_at	chr8p12-p11	protein tyrosine phosphatase activity	dual specificity phosphatase 4	3.9	5.07E-06
VGF	205586_x_at	chr7q22.1	neuropeptide hormone activity	VGF nerve growth factor inducible	3.7	0.0005
CDH4	206866_at	chr20q13.3	calcium ion binding	cadherin 4, type 1, R-cadherin (retinal)	3.3	0.008
NPTX1	204684_at	chr17q25.3	metal ion binding	neuronal pentraxin I	3.2	0.0009
DLK1	209560_s_at	chr14q32	calcium ion binding	delta-like 1 homolog (Drosophila)	3.1	0.02
ZIC1	206373_at	chr3q24	sequence-specific DNA binding transcription factor activity	Zic family member 1	2.9	0.004
CCND2	200951_s_at	chr12p13	protein kinase binding	cyclin D2	2.7	0.0009
CCNE1	213523_at	chr19q12	transcription co-activator activity /kinase activity	cyclin E1	2.7	0.016
TIE1	204468_s_at	chr1p34-p33	transmembrane receptor protein tyrosine kinase activity	tyrosine kinase with immunoglobulin-like and EGF-like domains 1	2.7	5.32E-06
ETV5[a]	203348_s_at	chr3q28	sequence-specific DNA binding transcription factor activity	ets variant 5	2.5	0.016
HEY1	218839_at	chr8q21	sequence-specific DNA binding transcription factor activity	hairy/enhancer-of-split related with YRPW motif 1	2.4	0.008
ETV1[a]	206501_x_at	chr7p21.3	sequence-specific DNA binding transcription factor activity	ets variant 1	2.1	0.004
WT1	206067_s_at	chr11p13	sequence-specific DNA binding transcription factor activity	Wilms tumor 1	2.1	0.10
HOXA5	213844_at	chr7p15.2	sequence-specific DNA binding transcription factor activity	homeobox A5	−2.1	3.67E-05
HOXC6	206858_s_at	chr12q13.3	sequence-specific DNA binding transcription factor activity	homeobox C6	−2.11	5.32E-06
SFRP1	202035_s_at	chr8p11.21	Wnt-protein binding	secreted frizzled-related protein 1	−2.31	0.0003

[Ω]selected from a 175 gene list;

* genes up-regulated by overexpression of CIC-DUX4 (Kawamura-Saito et al., 2006);

^{a} genes validated by qPCR.